Available online at www.sciencedirect.com
SCIENCE DIRECT®
Journal of Nuclear Materials 327 (2004) 175–181
journal of nuclear materials
www.elsevier.com/locate/jnucmat

Displacement damage in silicon carbide irradiated in fission reactors

H.L. Heinisch *, L.R. Greenwood, W.J. Weber, R.E. Williford

Pacific Northwest National Laboratory, 902 Battelle Blvd., P.O. Box 999, Richland, WA 99352, USA

Received 24 April 2003; accepted 9 February 2004

Abstract

Calculations are performed for displacement damage in SiC due to irradiation in the neutron environments of various types of nuclear reactors using the best available models and nuclear data. The displacement damage calculations use recently developed damage functions for SiC that are based on extensive molecular dynamics simulations of displacement events. Displacements per atom (DPA) cross sections for SiC have been calculated as a function of neutron energy, and they are presented here in tabular form to facilitate their use as the standard measure of displacement damage for irradiated SiC. DPA cross sections averaged over the neutron energy spectrum are calculated for neutron spectra in the cores of typical commercial reactors and in the test sample irradiation regions of several materials test reactors used in both past and present irradiation testing. Particular attention is focused on a next-generation high-temperature gas-cooled pebble bed reactor, for which the high-temperature properties of silicon carbide fiber-reinforced silicon carbide composites are well suited. Calculated transmutations and activation levels in a pebble bed reactor are compared to those in other reactors.
© 2004 Elsevier B.V. All rights reserved.

1. Introduction

Many concepts for advanced nuclear power reactors, Generation IV and beyond, call for much higher operating temperatures than current commercial reactors, either to significantly increase the efficiency of electric power production or to facilitate the production or co-production of hydrogen. While several advanced reactor designs employ SiC in fuel components to retain fission products, silicon carbide fiber-reinforced silicon carbide (SiC/SiC) composites also have outstanding high-temperature and nuclear properties that may make them well-suited for structural applications in such reactors. A crucial aspect of the development of SiC and SiC/SiC composites for nuclear applications is the evaluation of the effects of neutron irradiation on their mechanical and physical properties. Irradiating these materials in available irradiation environments, comparing results from various facilities, and extrapolating the material performance to use in new generations of power producing facilities requires that a standard method be used for quantitatively describing the cumulative displacement events in SiC under different neutron irradiation environments. The standard damage parameter for nuclear materials is displacements per atom (DPA), which incorporates information on the response of the material, i.e. displaced atoms, as well as the neutron spectrum and fluence to which it was exposed. The concept of DPA was initially developed for monatomic metals, where the definition of DPA is somewhat simpler than in multi-component ceramic materials where the various atom displacement energies are not easily measured. In the past few years significant progress has been made in modeling displacement damage in SiC using molecular dynamics computer simulations to determine displacement threshold energies [1] and employing improved models for stopping powers [2] based on the

* Corresponding author. Tel.: +1-509 376 3278; fax: +1-509 376 0418.
E-mail address: hl.heinisch@pnl.gov (H.L. Heinisch).

0022-3115/$ - see front matter © 2004 Elsevier B.V. All rights reserved.
doi:10.1016/j.jnucmat.2004.02.012

Table 1
Total DPA cross sections in barns for SiC as a function of neutron energy in MeV

E, MeV	σ_d, b
1.00×10^{-10}	$4.14\times10^{+00}$
1.00×10^{-09}	$1.31\times10^{+00}$
1.00×10^{-08}	6.84×10^{-01}
2.30×10^{-08}	4.58×10^{-01}
5.00×10^{-08}	3.44×10^{-01}
7.60×10^{-08}	2.80×10^{-01}
1.10×10^{-07}	2.30×10^{-01}
1.70×10^{-07}	1.88×10^{-01}
2.50×10^{-07}	1.54×10^{-01}
3.80×10^{-07}	1.27×10^{-01}
5.50×10^{-07}	1.04×10^{-01}
8.40×10^{-07}	8.43×10^{-02}
1.28×10^{-06}	6.86×10^{-02}
1.90×10^{-06}	5.66×10^{-02}
2.80×10^{-06}	4.61×10^{-02}
4.20×10^{-06}	3.70×10^{-02}
6.30×10^{-06}	3.11×10^{-02}
9.20×10^{-06}	2.57×10^{-02}
1.30×10^{-05}	2.10×10^{-02}
2.10×10^{-05}	1.72×10^{-02}
3.00×10^{-05}	1.42×10^{-02}
4.50×10^{-05}	1.10×10^{-02}
6.90×10^{-05}	9.46×10^{-03}
1.00×10^{-04}	8.02×10^{-03}
1.30×10^{-04}	7.03×10^{-03}
1.70×10^{-04}	6.20×10^{-03}
2.20×10^{-04}	9.53×10^{-02}
2.80×10^{-04}	3.56×10^{-01}
3.60×10^{-04}	$1.60\times10^{+00}$
4.50×10^{-04}	$1.34\times10^{+00}$
5.70×10^{-04}	$1.10\times10^{+00}$
7.60×10^{-04}	$2.86\times10^{+00}$
9.60×10^{-04}	$3.74\times10^{+00}$
1.28×10^{-03}	$2.91\times10^{+00}$
1.60×10^{-03}	$4.32\times10^{+00}$
2.00×10^{-03}	$6.89\times10^{+00}$
2.70×10^{-03}	$9.07\times10^{+00}$
3.40×10^{-03}	$1.06\times10^{+01}$
4.50×10^{-03}	$1.38\times10^{+01}$
5.50×10^{-03}	$1.90\times10^{+01}$
7.20×10^{-03}	$2.36\times10^{+01}$
9.20×10^{-03}	$2.69\times10^{+01}$
1.20×10^{-02}	$3.06\times10^{+01}$
1.50×10^{-02}	$3.91\times10^{+01}$
1.90×10^{-02}	$4.91\times10^{+01}$
2.50×10^{-02}	$5.90\times10^{+01}$
3.20×10^{-02}	$7.26\times10^{+01}$
4.00×10^{-02}	$8.86\times10^{+01}$
5.20×10^{-02}	$1.79\times10^{+02}$
6.60×10^{-02}	$1.51\times10^{+02}$
8.80×10^{-02}	$1.54\times10^{+02}$
1.10×10^{-01}	$1.54\times10^{+02}$
1.30×10^{-01}	$1.51\times10^{+02}$
1.60×10^{-01}	$4.67\times10^{+02}$
1.90×10^{-01}	$6.32\times10^{+02}$
2.20×10^{-01}	$5.04\times10^{+02}$
2.50×10^{-01}	$4.62\times10^{+02}$
2.90×10^{-01}	$4.16\times10^{+02}$
3.20×10^{-01}	$4.08\times10^{+02}$
3.60×10^{-01}	$4.53\times10^{+02}$
4.00×10^{-01}	$4.20\times10^{+02}$
4.50×10^{-01}	$4.70\times10^{+02}$
5.00×10^{-01}	$4.89\times10^{+02}$
5.50×10^{-01}	$5.28\times10^{+02}$
6.00×10^{-01}	$4.67\times10^{+02}$
6.60×10^{-01}	$4.78\times10^{+02}$
7.20×10^{-01}	$5.20\times10^{+02}$
7.80×10^{-01}	$8.01\times10^{+02}$
8.40×10^{-01}	$5.70\times10^{+02}$
9.20×10^{-01}	$7.22\times10^{+02}$
$1.00\times10^{+00}$	$5.19\times10^{+02}$
$1.20\times10^{+00}$	$5.90\times10^{+02}$
$1.40\times10^{+00}$	$6.08\times10^{+02}$
$1.60\times10^{+00}$	$6.03\times10^{+02}$
$1.80\times10^{+00}$	$8.27\times10^{+02}$
$2.00\times10^{+00}$	$6.02\times10^{+02}$
$2.30\times10^{+00}$	$6.60\times10^{+02}$
$2.60\times10^{+00}$	$7.10\times10^{+02}$
$2.90\times10^{+00}$	$7.09\times10^{+02}$
$3.30\times10^{+00}$	$6.92\times10^{+02}$
$3.70\times10^{+00}$	$9.96\times10^{+02}$
$4.10\times10^{+00}$	$7.96\times10^{+02}$
$4.50\times10^{+00}$	$8.46\times10^{+02}$
$5.00\times10^{+00}$	$7.04\times10^{+02}$
$5.50\times10^{+00}$	$7.01\times10^{+02}$
$6.00\times10^{+00}$	$6.49\times10^{+02}$
$6.70\times10^{+00}$	$6.42\times10^{+02}$
$7.40\times10^{+00}$	$9.20\times10^{+02}$
$8.20\times10^{+00}$	$7.31\times10^{+02}$
$9.00\times10^{+00}$	$8.08\times10^{+02}$
$1.00\times10^{+01}$	$7.99\times10^{+02}$
$1.10\times10^{+01}$	$8.57\times10^{+02}$
$1.20\times10^{+01}$	$8.86\times10^{+02}$
$1.30\times10^{+01}$	$8.79\times10^{+02}$
$1.40\times10^{+01}$	$8.70\times10^{+02}$
$1.50\times10^{+01}$	$9.21\times10^{+02}$
$1.60\times10^{+01}$	$9.00\times10^{+02}$
$1.70\times10^{+01}$	$8.72\times10^{+02}$
$1.80\times10^{+01}$	$9.36\times10^{+02}$
$1.90\times10^{+01}$	$9.20\times10^{+02}$
$2.00\times10^{+01}$	

In these 100 group cross sections the energy values are the lower bin energies and the cross sections are averaged over each group.

methodology of Huang and Ghoniem [3]. This information has been utilized for the calculation of DPA cross sections for SiC as a function of neutron energy [4].

To be most useful, the DPA damage parameter should be defined and calculated the same way by all concerned, and preferably for all past, present and future experiments, models and analyses. To that end, we include here the DPA cross sections as a function of

neutron energy for SiC in tabulated form, Table 1. This function, along with neutron flux and energy spectrum information, can be used to calculate the DPA value for SiC in any neutron irradiation environment. As examples, we include DPA cross sections averaged over the neutron energy spectrum for a variety of existing materials test reactors, commercial reactors, and a high-temperature, gas-cooled, pebble bed reactor (Generation III+).

Radiation-induced transmutations are a consequence of neutron irradiation that can be equally as important as displacement damage in determining the suitability of a material for nuclear applications. Concentrations of transmutants also depend on the neutron flux and energy spectrum at the irradiation location. Examples of transmutation concentration levels in SiC irradiated in different reactor spectra are also presented and discussed.

2. Displacements per atom

Displacements per atom is a calculated measure of radiation damage that reflects not only the dose and type of irradiation, but also includes some measure of the material's response to the irradiation. DPA is a measure of the 'damage energy' deposited in the material by the irradiating particles in terms of how many atoms could possibly be permanently displaced from their lattice sites to stable interstitial sites by this damage energy. Because of 'cascade' effects, DPA is not in general a measure of the residual crystal lattice defects actually created in a material. In each individual radiation damage event, the primary knock-on atom (PKA, an atom that has received kinetic energy through interaction with a neutron or other higher energy particle) imparts energy to neighboring atoms, producing a cascade of collisions, if it has enough energy to do so. Within the affected volume of a typical high-energy collision cascade, many atoms are displaced significantly from their lattice sites, creating a near-molten zone in the crystal. However, within a few picoseconds, many of the displaced atoms return to vacant sites, thereby healing much of the damage. The actual number of lattice defects ('permanently' displaced atoms) remaining after the cascade region cools is usually a small fraction of the atoms initially displaced in the cascade. This fraction is often referred to as the 'efficiency' of defect production relative to the calculated DPA value, and it can vary considerably depending on the material, the source of irradiation and the irradiating conditions. For typical nuclear reactor applications and doses, the actual damage in the irradiated materials scales with the calculated DPA. Thus, DPA has been found to be an extremely useful damage parameter for correlating the effects of radiation damage in the same material irradiated in different nuclear reactor environments, and it is the standard damage parameter for nuclear structural materials.

The original model for displacement damage, developed initially for simple metals, is due to Kinchin and Pease [5], and the standard formulation of it by Norgett et al. [6], often referred to as the 'NRT' model, is

$$\begin{aligned} \nu(T) &= 0 \quad T < E_{\mathrm{d}}, \\ &= 1 \quad E_{\mathrm{d}} < T < 2E_{\mathrm{d}}, \\ &= 0.8T/2E_{\mathrm{d}} \quad T > 2E_{\mathrm{d}}, \end{aligned} \tag{1}$$

where $\nu(T)$ is the number of displaced atoms produced by a recoil atom of energy E and damage energy T, and E_{d} is the average threshold displacement energy for an atom in the metal. Damage energies $T(E)$ can be calculated for each recoil energy E using an analytic expression due to Robinson [7]. The threshold displacement energy E_{d} can be determined experimentally for simple metals. For more complicated materials, such as polyatomic materials or those with complex crystal structures, where there may be several different displacement energies, the values of E_{d} are best determined with the aid of computer simulations. The energies required to displace Si and C atoms from their lattice sites to interstitial positions in SiC have been determined using atomic-scale molecular dynamics and first principles calculations [1]. The values of displacement energies averaged over all directions in SiC have been determined to be 20 eV for C and 35 eV for Si, and it is recommended that these values be used universally for calculating DPA in irradiated SiC [8]. There are actually four minimum recoil damage energies required to create displacements in SiC, depending on the projectile/target combinations: 41 eV (C/Si), 35 eV (Si/Si), 24 eV (Si/C) and 20 eV (C/C) [4]. The minimum recoil damage energies for the C/Si and Si/C projectile/target combinations are easily derived from the self-ion combinations since, for example, a C atom must have kinetic energy of at least 41 eV to provide the 35 eV to a Si atom that is necessary to displace it.

Treating polyatomic materials introduces other complications to the formulation of damage functions due to the interactions among sublattices. Thus, in the present work displacement functions for polyatomic materials, $\nu_{ij}(E)$, for the average number of atoms of type j initiated by a PKA of type i and energy E, were obtained by numerical solutions of the coupled integro-differential equations for $\nu_{ij}(E)$ devised by Parkin and Coulter [9–11] and using the displacement energies discussed above. Atomic scattering cross sections based on the Ziegler, Biersack, and Littmark (ZBL) universal screening potential [12] were used in the calculation of the displacement functions, and the electronic stopping powers used in the calculations were generated from the

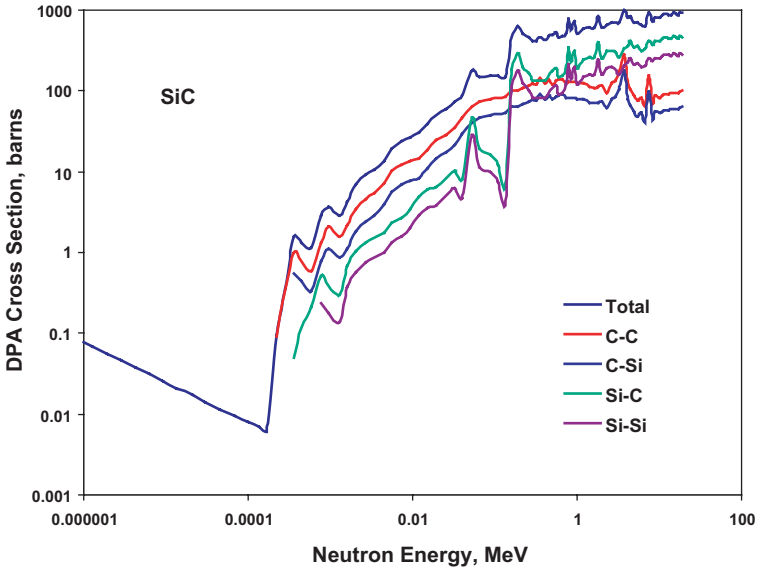

Fig. 1. Total DPA cross sections in barns for SiC as a function of neutron energy in MeV. The individual contributions from each PKA-target atom type are also shown. The (n,gamma) contributions to these individual sub-reaction cross sections are not included, so they stop at the threshold energies. The significant dips in the Si–C and Si–Si sub-reaction cross sections are due to the large, broad resonance structure for Si spanning the 0.1–0.2 MeV region.

SRIM 2000 electronic stopping power database [13]. The use of these representations of the scattering and stopping powers in the calculation of displacement functions for SiC is demonstrated and discussed in Ref. [2].

The damage functions $\nu_{ij}(T)$ are integrated over the PKA damage energy spectrum for a neutron of energy E_n in the material, to yield the Si, C and total (Si + C) displacement cross sections for neutrons of energy E_n. This has been done for SiC using the SPECOMP code [14], and the results for total DPA cross sections are tabulated in Table 1 and shown graphically in Fig. 1 as a function of E_n.

3. Neutron spectra

To examine the effects of the neutron energy spectrum on DPA cross sections in SiC, spectrally averaged total DPA cross sections for SiC have been calculated for a variety of neutron environments, including existing commercial and research reactors, as well as a high-temperature gas-cooled fission reactor (GCR). The GCR neutron flux is significantly softer and lower than for the other reactors, primarily because of its low power density design.

Graphite-moderated GCRs were designed as early as the 1960s, and even constructed and operated as Generation I prototype reactors. The present GCR concepts are considered as Generation III+, i.e., evolutionary designs for commercial reactors of the next few decades [15]. Present designs comprise two primary concepts exemplified by their core configurations: the modular pebble bed reactor (MPBR) having graphite spheres arranged in a 'pebble bed' and the gas turbine modular helium reactor (GT-MHR) having hexagonal graphite blocks stacked in a prismatic core. In both configurations the oxide fuel is in the form of ceramic coated microspheres dispersed throughout the graphite pebbles or blocks.

The GCR neutron energy spectrum used in the present work is for a MPBR [16]. The MPBR concept is based on a 265 MWth reactor with a graphite-moderated, helium-cooled 'core' that consists of 330 000 spheres of graphite, each of which is about 6 cm in diameter and contains a distribution of thousands of microspheres of uranium oxide reactor fuel coated by layers of graphite and SiC, which provides fuel containment. Additional moderation is obtained from a distribution of 110 000 unfueled graphite spheres arranged in the pebble bed. The MPBR design has a total neutron flux of 1.25×10^{14} n/cm^2 s, which is about 1/3 the flux in a typical commercial pressurized water reactor (PWR) and up to more than an order of magnitude less than the fluxes in some materials test reactors such as the High Flux Isotope Reactor (HFIR). More importantly, the MPBR has a significantly softer neutron energy spectrum due to the low power density of its design.

4. Spectrally averaged DPA cross sections

When the displacement function is integrated over the flux spectrum of neutron energies for a given reactor location, the result is a cross section for total DPA in SiC averaged over the neutron energy spectrum. The total DPA obtained by a SiC specimen in a specific irradiation is then the product of the spectrally averaged DPA cross section for SiC and the total neutron fluence received by the specimen. Table 2 contains spectrally averaged total DPA cross sections for SiC at in-core positions for a variety of test reactors, a typical commercial PWR, a typical commercial boiling water reactor (BWR), and the MPBR. This table also contains DPA cross sections for pure Fe in the same reactor locations as a comparison. Among the different reactors, the variation in the spectrally-averaged DPA cross sections for SiC is different from that of Fe. In general, it is not advisable to try estimating the DPA for one material based on the DPA calculated for another material in the same neutron spectrum.

The DPA cross section for SiC in the MPBR is small compared to those of the commercial and test reactors, which have DPA cross sections about 1.5 to 4 times larger. The differences in DPA cross sections are due entirely to the differences in the neutron energy spectra, especially in the relative numbers of fast neutrons ($E > 0.1$ MeV), which produce essentially all the displacement damage. The fractions of total neutrons that have energies greater than 0.1 MeV are 0.19 for MPBR, 0.28 for the mixed-spectrum reactor HFIR-PTP, 0.41 for a typical PWR, and 0.93 for the midplane of the liquid metal-cooled fast reactor EBR-2. (This measure of relative neutron energy spectrum 'hardness' is somewhat crude, since it does not take into account the specific shape of the spectrum.)

Table 2
Spectrally averaged total DPA cross sections, σ_{DPA}, in barns for SiC in various fuels and materials test reactor positions, typical commercial reactors, and a pebble bed reactor design

Reactor	Position	σ_{DPA}, barns	
		Fe	SiC
MPBR	Core/He coolant	117	113
FFTF	MOTA above core +121 cm	103	149
HFIR	PTP mid	191	158
FFTF	MOTA below core −67.7 cm	132	181
HFR	D2	255	234
ATR	Midplane (no Gd)	302	260
PWR	Midplane	311	262
HFR	C5	300	263
BWR	Midplane	303	265
HFIR	RB*(Hf liner)	280	276
FFTF	MOTA midplane	267	324
ATR	Midplane (w/Gd)	401	344
EBR-2	Midplane	390	423

Values for pure Fe are shown for comparison to typical metals. Listed in order of increasing values of σ_{DPA} for SiC.

Table 3
Displacement damage rates in DPA per effective full power year (DPA/efpy) for SiC in several fuel and materials test reactors, commercial reactors, and a pebble bed reactor design

Reactor	Position	DPA/efpy	
		Fe	SiC
MPBR	Core/He coolant	0.46	0.44
BWR	Midplane	2.8	2.4
PWR	Midplane	3.7	3.1
HFR	C5	12	11
ATR	Midplane	14	12
EBR-2	Midplane	25	27
HFIR	PTP mid	33	28
FFTF	MOTA midplane	43	53

Values for pure Fe are shown for comparison to typical metals. Listed in order of increasing values for SiC.

The damage rate in a material, i.e. the rate of DPA production during an irradiation, is obtained by multiplying the total neutron flux in the irradiation environment by the spectrally averaged DPA cross section. Table 3 contains the DPA damage rates per effective full power year (DPA/efpy) corresponding to the neutron fluxes in the reactor core positions listed in Table 2. The damage rates for SiC in commercial PWR and BWR reactors are about 5 times higher than the damage rates in the MPBR, reflecting the low neutron flux and low power density of the MPBR. In the test reactors, designed to achieve high neutron fluxes, damage rates are more than an order of magnitude greater than the 0.44 DPA/efpy in the MPBR, thus they could be used to quickly irradiate test materials to MPBR lifetime doses. However, damage correlations between results from test reactors and a conceptual MPBR would also have to consider the potential effects of the differing damage rates, as well as effects of any differences in irradiation temperature.

5. Transmutations

Neutron irradiation-induced transmutations result in the presence of both radioactive and stable transmutant elements in the irradiated material. In general, as the neutron irradiation proceeds, the composition of the irradiated material can change due to the addition or depletion of solutes and impurities through radiation-induced transmutations, as well as becoming radioactive. Transmutations can also lead to stoichiometric changes in compounds and alloys, if the various elements 'burn out' at significantly different rates. Since the transmutant elements themselves are subject to transmutation under

Table 4
Concentrations of elements in SiC produced by neutron irradiation-induced transmutations after irradiation in the MPBR for 10 full power years (4.4 dpa)

Element	MPBR		HFIR-PTP, appm/dpa
	appm	appm/dpa	
P	36	8.2	6.1
H	8.0	1.8	3.3
He	5.8	1.3	2.5
Mg	3.6	0.8	1.5
Be	1.5	0.3	1.4

The transmutation per dpa is compared with that for SiC in HFIR-PTP.

continuing irradiation, some changes in composition due to transmutation are, in general, non-linear with irradiation dose. The transmutation rates of the various isotopes in the material depend on the cross sections for the nuclear reactions that produce them, which are a function of the neutron energy.

Calculations of transmutation and activation were performed using the REAC*3 code [17] for pure SiC irradiated for 10 full power years (with a total damage accumulation of 4.4 DPA) in the MPBR. During that exposure significant concentrations of five elements, P, He, H, Mg, and Be, were produced by transmutation, and the results are shown in Table 4. The concentrations of transmutants are listed in atomic parts per million (appm), and the ratio of transmutation relative to displacement damage (appm/DPA) is also shown.

Concentrations of the transmutants in SiC listed in Table 4 increase linearly with dose over 10 full power years in the MPBR spectrum. The radiation-induced impurity concentrations exceed the intrinsic impurity levels for these elements found in ultra-pure electronics-quality CVD SiC by factors of 250–1000. However, the concentrations of transmutant elements listed in Table 4 are extremely low compared to the concentrations of intrinsic impurities typically measured in the fibers or matrix of unirradiated SiC/SiC composites intended for structural applications, which are considerably more impurity-laden.

For comparison with an operating research reactor, transmutation calculations were also made for SiC in the neutron spectrum of HFIR-PTP, as shown in Table 4. The primary transmutants in this mixed-spectrum reactor are the same elements as those in the MPBR, and the concentration levels of transmutant elements per DPA are quite similar.

Induced radioactivity is generally extremely low for pure SiC irradiated in any neutron environment. In MPBR after 10 efpy of irradiation and 4 days of cooling, pure SiC has a residual decay rate of about 4×10^{-4} Ci/g. This activity is due primarily to ^{32}P, which is a beta emitter. The gamma dose rate at this time is 3×10^{-11} R/h/cm^3 at 1 m due to several short-lived gamma emitters. After cooling a year, the decay rate has decreased to 1×10^{-6} Ci/g, dominated by ^{14}C, while the gamma dose rate is 5×10^{-14} R/h/cm^3 at 1 m, due to the long-lived ^{26}Al produced from Si by a two-step reaction. Most of the induced radioactivity in SiC used for structural materials in nuclear reactors will come from activation of the impurities inevitably present in the base material or introduced during fabrication.

6. Conclusions

The DPA cross sections in Table 1 represent the latest and best knowledge about damage production in SiC. We encourage the adoption of these cross sections as the standard to be used for calculating radiation damage production in DPA for all neutron-irradiated SiC samples, including those in past irradiations if possible.

SiC, especially in the form of SiC/SiC composites, is a potentially useful material for high temperature structural applications in nuclear energy. SiC is an inherently low-activation material, with even lesser effects in a soft neutron spectrum such as the MPBR. Because of the low doses involved, transmutations are probably not a significant concern for SiC (or other materials) in the MPBR, except for perhaps the appm levels of He and H. While the average concentration of these gas atoms is small, their high mobility means they could possibly concentrate at undesirable locations in the microstructure. Burnout of SiC is insignificant in MPBR, and it is not a significant concern for SiC in test reactors and commercial reactors.

Acknowledgements

The authors are indebted to Dr J. Stephen Herring of INEEL for numerical values of the MPBR reactor neutron spectrum. This work was supported in part by the US Department of Energy Offices of Nuclear Energy and Basic Energy Sciences.

References

[1] R. Devanathan, W.J. Weber, J. Nucl. Mater. 278 (2000) 258.
[2] W.J. Weber, R.E. Williford, K.E. Sickafus, J. Nucl. Mater. 244 (1997) 205.
[3] H. Huang, N. Ghoniem, J. Nucl. Mater. 199 (1993) 221.
[4] H. Heinisch, L.R. Greenwood, W.J. Weber, R.E. Williford, J. Nucl. Mater. 307–311 (2002) 895.
[5] G.H. Kinchin, R.S. Pease, Rep. Prog. Phys. 18 (1955) 1.
[6] M.J. Norgett, M.T. Robinson, I.M. Torrens, Nucl. Eng. Des. 33 (1975) 50.

[7] M.T. Robinson, in: Proceedings of British Nuclear Energy Soc., UKAEA, London, 1970, p. 364.
[8] R. Devanathan, W.J. Weber, F. Gao, J. Appl. Phys. 90 (2001) 2303.
[9] D.M. Parkin, C.A. Coulter, J. Nucl. Mater. 101 (1981) 261.
[10] D.M. Parkin, C.A. Coulter, J. Nucl. Mater. 103&104 (1981) 1315.
[11] D.M. Parkin, C.A. Coulter, J. Nucl. Mater. 117 (1983) 340.
[12] J.F. Zeigler, J.P. Biersack, U. Littmark, The Stopping and Range of Ions in Solids, Pergamon, New York, 1985.
[13] J.F. Zeigler, SRIM-2000, code and manuals available on the Internet at http://www.srim.org, (2001).
[14] L.R. Greenwood, ASTM STP 1001 (1989) 598.
[15] G.H. Marcus, A.E. Levin, Phys. Today 55 (2002) 54.
[16] Proliferation resistant advanced nuclear fuel cycles, Annual project Report, INEEL/EXT-2000-01048, July 2000.
[17] F.M. Mann, D.E. Lessor, REAC*3 Nuclear Data Libraries, in: Proceedings for International Conference on Nuclear Data for Science and Technology, Julich, Germany, May (1991).